

LRP 710/01

October 2001

**Diagnostics Neutral Beam Injector at  
the TCV Tokamak**

J. Mlynar, A.N. Shukaev, P. Bosshard,  
B.P. Duval, A.A. Ivanov, M. Kollegov,  
V.V. Kolmogorov, X. Llobet, R.A. Pitts  
& H. Weisen

# Diagnostics Neutral Beam Injector at the TCV Tokamak

J. Mlynar, A.N. Shukaev<sup>1</sup>, P. Bosshard, B. Duval, A.A. Ivanov<sup>1</sup>, M. Kollegov<sup>1</sup>,  
V.V. Kolmogorov<sup>1</sup>, X. Llobet, R.A. Pitts and H. Weisen

Centre de Recherche en Physique des Plasmas, EPFL, Lausanne, Switzerland

<sup>1</sup>Budker's Institute of Nuclear Physics, Novosibirsk, Russia

**Abstract.** Within this report we summarize the technical and experimental effort made on diagnostics neutral beam injector (DNBI) which was installed at tokamak TCV last year. Basic components of DNBI are reviewed, its remote control is presented in more detail. Profile and attenuation studies are referred to. First experimental results obtained with DNBI, which led to a decision to upgrade the machine, are discussed in the last section.

## 1. Introduction

Fusion oriented high temperature plasma experiments often use powerful neutral beams not only for additional plasma heating, but also for purely diagnostics purpose. The diagnostics neutral beams are not supposed to influence the plasma parameters significantly. Unlike the heating beams, they are installed almost perpendicularly to the plasma to allow high radial resolution and are modulated in time to allow subtraction of the passive signal. This report reviews the basic characteristics and first results obtained with the diagnostic beam neutral injector (DNBI) from Budker's Institute of Nuclear Physics (BINP, Novosibirsk) which was commissioned last year on TCV at the CRPP EPFL.

TCV (Tokamak à Configuration Variable, see Fig.1) strength in the research of magnetically confined hot plasmas is its ability to produce highly shaped plasmas with elongation up to 2.8 achieved to date. The toroidal chamber has a major radius  $R = 0.88$  m and a minor radius  $r = 0.25$  m. Together with TCV extended capabilities of plasma control, investigation of the effects of plasma shaping on confinement and stability is possible [1]. Deuterium plasma discharges with toroidal current  $I < 1.2$  MA are confined for approx. 2 s in a toroidal field  $B_T < 1.54$  T. Besides, a powerful electron cyclotron heating and current drive system (ECH, ECCD) with max. 4.5 MW of additional heating has been installed at TCV, resulting in central plasma electron temperature increase to above 10 keV [1]. The plasma electron temperature profiles are measured by a 35-channel Thomson scattering system with 60 Hz repetition rate. So far there is however little knowledge about the ion temperature behavior on TCV.

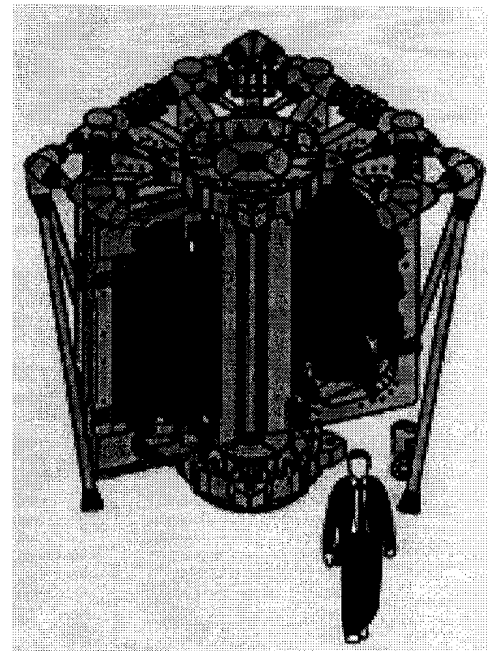


*Fig. 1: TCV tokamak cross-section.  
For more details on TCV see its website  
<http://crppwww.epfl.ch/tcv/>*

The primary task of the DNBI is to provide together with CXRS (Charge eXchange Recombination Spectroscopy, see Fig. 2) a diagnostic tool for the local measurements of TCV plasma ion temperature from the impurity (carbon) line Doppler broadening. However, diagnostic beams can deliver further information on plasma characteristics along the beam path (for details see e.g. [2]): the concentrations of different impurities (from absolute measurements of intensities of their lines), collective plasma motion from the Doppler shift of spectral lines and local measurements of safety factor  $q$  (magnetic field helicity) from lines splitting and/or polarization. The latter application, known as Motional Stark Effect (MSE) diagnostics [3], is however very demanding on the signal processing. It may be developed on TCV only after successful implementation of CXRS.

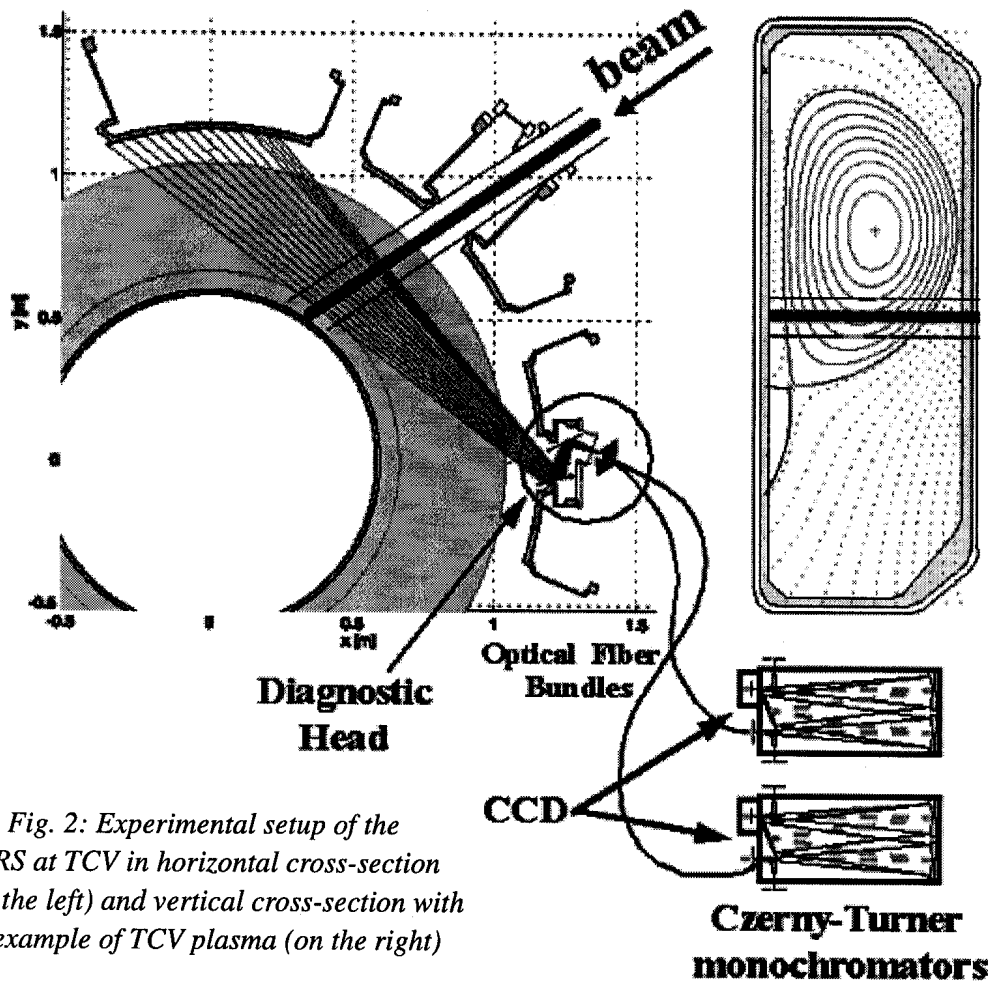


Fig. 2: Experimental setup of the CXRS at TCV in horizontal cross-section (on the left) and vertical cross-section with an example of TCV plasma (on the right)

An overview of the parameters of the DNBI, its experimental set-up and basic supplies will be presented in the following section of this report. The novel remote control system is outlined in the third section. Next we briefly present the results of beam profile and attenuation studies. In the fifth section, the first DNBI experimental results are discussed. As a conclusion, the necessity of the DNBI upgrade to higher local current density is stated.

## 2. DNBI characteristics, principles and supplies

According to the technical specifications, the DNBI must provide a neutral beam with the following characteristics:

- beam energy range: 20-50 keV (optimised for 50 keV),
- equivalent neutral beam current: 0.5 A at 50 keV within  $\phi$  10 cm diameter at 4 m from the source,

- modulation: on-time range 1 ms to 2 s, minimal off-time 2 s,
- beam focus near the centre of the TCV plasma, beam divergence 0.6-0.7°,
- beam components: 73%  $H_1^+$ , 20%  $H_2^+$  and 7%  $H_3^+$  in beam source electrical current.

The injector principle is presented in Fig. 3.

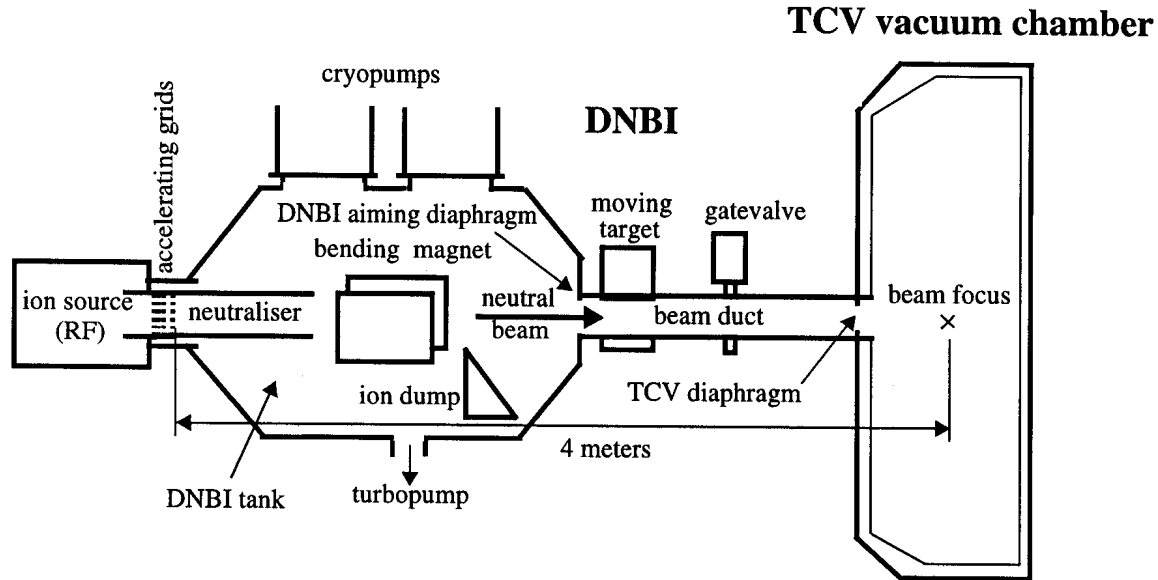


Fig. 3: Principal scheme of the diagnostic neutral beam injector at tokamak TCV

The RF ion source produces a homogenous hydrogen plasma, which serves as the source of ions for the beam. The source plasma is driven by 5 kW, 4.6 MHz RF generator. The support systems of the source include water cooling, hydrogen gas supply, gas puff control and plasma ignition system. The beam extracted from the ion source consists of approx. 73% of protons, 20% of  $H_2^+$  and 7% of  $H_3^+$  (in beam current). Four molybdenum accelerating grids with 163 circular apertures within a 70 mm diameter assure proton acceleration and optimal collimation of the beam. The first (plasma) and the second (extracting) grids are power supplied by a high voltage modulator (max. 50 kV and 44.5 kV, 2A), the third (accelerating) grid is biased at -450 V, the fourth grid is grounded. The four grids are spherical with a radius of 4 m, so that the beam is focused to the TCV plasma centre. The grid support frame is water cooled. For more details on ion source and accelerating grids see [4].

The neutraliser tube keeps a suitable hydrogen gas density for the beam neutralisation via charge exchange collisions. The neutralising gas flows to the water-cooled tube from the ion source through the grids. Approx. 50% of accelerated protons are neutralised at 50 kV, the  $H_2^+$  are dissociated and then neutralised with approx. 78% efficiency and the  $H_3^+$  component is after dissociation neutralised with 85% efficiency. Consequently, ratio of the resulting neutral beam flux to the total ion extracted current is approx. 36% in the full-energy component, 31% in the half-energy component and 18% in the E/3 component.

A bending magnet deflects non-neutralised particles of the accelerated beam (approx. 50% of the total extracted current) to the residual ion dump. Both the bending magnet and the ion dump must be water-cooled. The bending magnet has a special 12V/650A power source.

All the non-accelerated gas particles must be evacuated with high pumping speed in order to prevent their influx to the TCV vacuum chamber. Two liquid He cryopumps, each with pumping speed  $24 \text{ m}^3\text{s}^{-1}$ , guarantee maximum pressure at the beam duct  $<10^{-3} \text{ Pa}$  during beam operation. Liquid He (35 l) and a thermally isolating liquid  $N_2$  (35 l) supply are necessary for the operation of each of the two

cryopumps. The liquid nitrogen refill has been automated, a weekly liquid helium refill is provided from a dewar. The dewar is pressurized by He gas line, and the cryopumps He exhaust is thermalised by water cooled heaters during the LHe refill. Furthermore, the cryosorbing surfaces are conditioned on a daily basis by a puff of a N<sub>2</sub> gas into the DNBI tank.

A standard vacuum pumping system with primary pump and turbopump is necessary for preliminary pumping for cryopumps regeneration. During the regeneration, the cryosorbed ice layers evaporate by warming up to room temperature. The released hydrogen and nitrogen gases are evacuated by the turbopump. The turbopump also assists the cryopumps by pumping out rare gases, e.g. helium gas which can get to the DNBI tank from TCV glow discharge residuals. The vacuum system is equipped with an independent power supply and remote control.

At the exit of the injector tank an annular aiming diaphragm is installed to limit the beam diameter and to measure the beam edge intensity using four secondary emission detectors. A retractable (moving) target is installed on the beam duct, which intercepts the beam when it is operated independently on TCV. It consists of nested copper rings, each with a thermocouple, allowing beam profile measurements. Both the aiming diaphragm and the moving target are water cooled.

The connecting tube to the TCV includes bellows, electric insulation and four flanges which allow future beam instrumentation to be added. The main vacuum gatevalve uses pressurized air for its remote control. Four thermocouples have been installed in the TCV inner wall opposite of the beam duct to monitor the carbon tiles temperature in the neutral beam strike area.

Safety systems prevent beam operation when the system is not ready or when it could cause damage. For example, either the moving target must be closed or the main gatevalve opened, the cooling water must circulate, etc. The main gatevalve can be open only if the vacuum on both sides is sufficient.

### 3. DNBI remote control

A challenge for the DNBI manufacturer was the interface between the TCV control system (TCVCS) and the injector control system. One of the fundamental principles of the TCVCS is its full centralisation. All TCV system and diagnostics facilities must be controllable from a single cluster of VMS/Alpha machines. It was originally agreed with the DNBI manufacturer that TCVCS would directly control and read all the DNBI inputs and outputs. However, in order to accomplish independent DNBI tests and commissioning, the machine was equipped with a CAMAC hardware, which was controlled by a PC with dedicated Java routines and autonomous GUI control window.

For simplicity and higher flexibility, it was finally decided that this control scheme would be preserved and that a special Java routine would be developed to establish communication between the DNBI control software and the VMS/Alpha machines via TCP/IP. This idea was successfully implemented by the DNBI manufacturer. The DNBI control database and control window in TCVCS were developed in parallel at CRPP.

The scheme of the final form of the DNBI control system is in fig. 4. The DNBI control software, which was written in Java for historical reasons, consists of three main parts:

- hardware drivers corresponding to the CAMAC modules,
- workflow control processes, which manage all necessary sequences for the DNBI operation, including the PC GUI control window, and
- interface to the TCVCS system, which allows remote control of the DNBI software by exchanging the control and acquisition data with TCVCS.

Another important part of the DNBI control is the timing. The CAMAC timers as well as other beam parameters are pre-set by the DNBI control software. Once the DNBI shot is triggered, no fundamental control of the beam is left to the software, i.e. the shot is driven by CAMAC modules which are inherently faster and have a defined time response. The shot trigger ("start command") may come either from the software control system (under the control regime "test") or externally from TCVCS to DNBI CAMAC via optical fibre (under the control regime "TCV"). A survey of the DNBI timing is given in fig. 5.

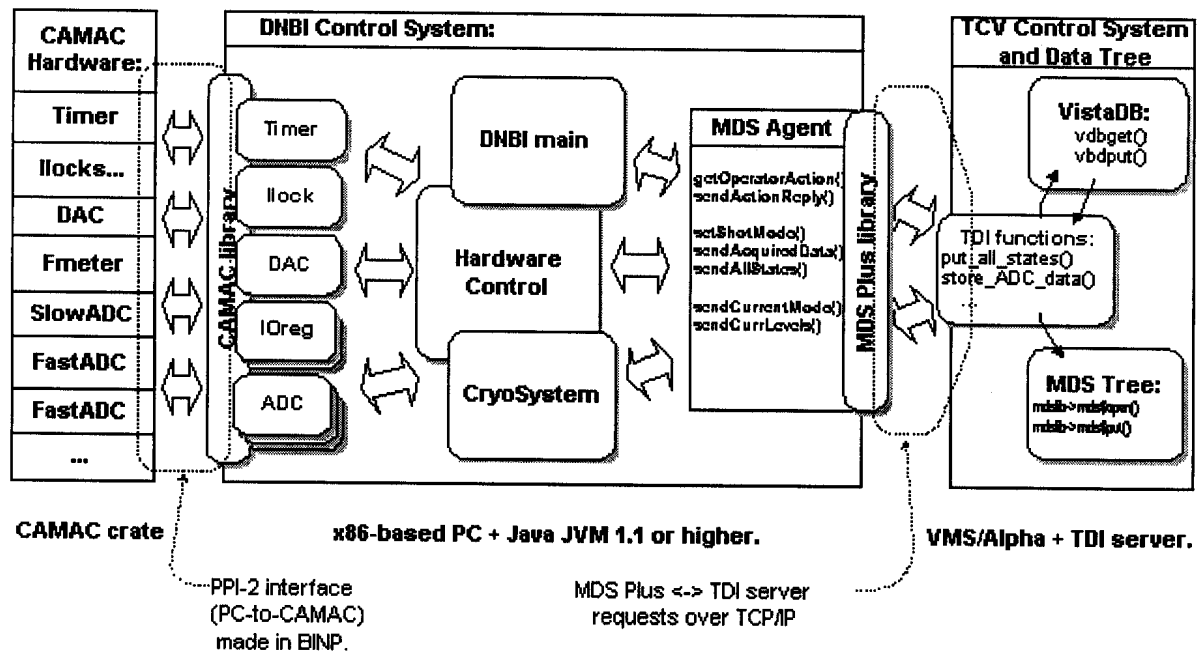


Fig. 4: Elements of the DNBI remote control system

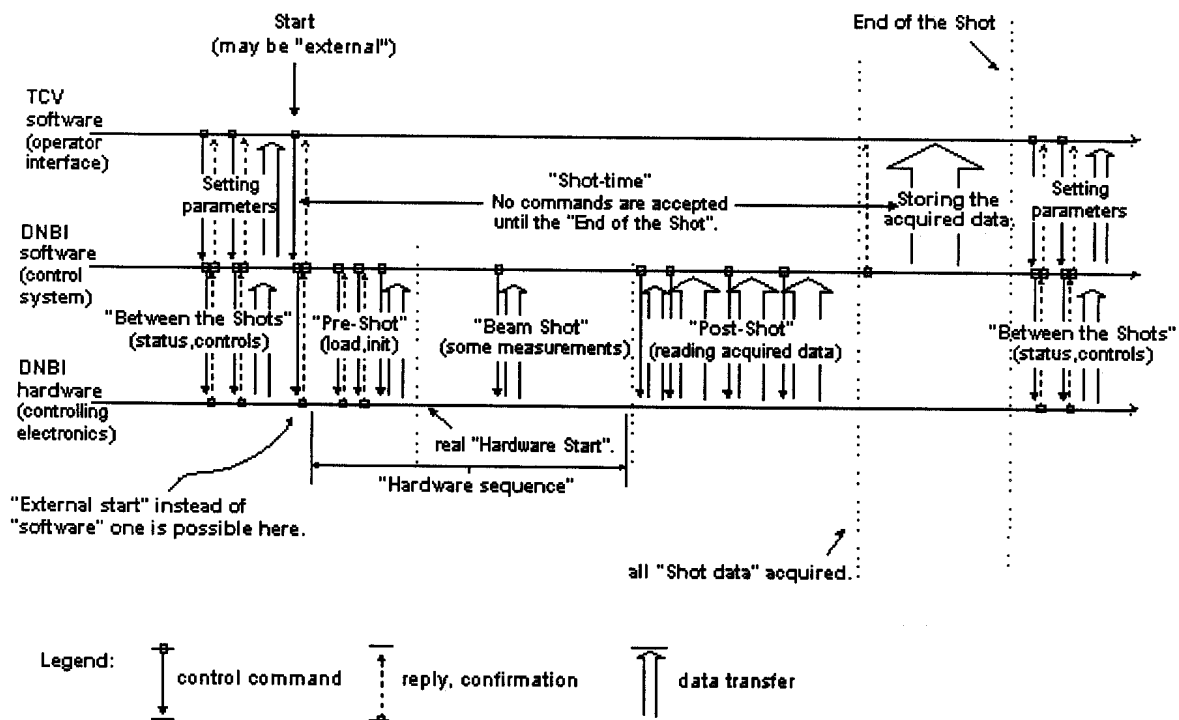


Fig. 5: Timing of a single DNBI shot

#### 4. DNBI profile and attenuation

As mentioned in the introduction, a reliable model of the beam profile and intensity is necessary for the absolute measurements of the active CX emission. This has been studied in detail in ref. [5]. Three important results were presented in this reference:

1. The following approximate formula has been derived for the beam current density profile in vacuum with the ion source radius  $a$  and beam divergence  $\vartheta$

$$j(z, r) = j(z, 0) \cdot \exp\left(-\frac{\pi}{I} j(z, 0) \cdot r^2\right) \quad \text{where}$$

$$j(z, 0) = \frac{I}{\pi a^2} \frac{z^{*2}}{z^2} \left(1 - \exp\left(-\frac{a^2}{z^{*2} \tan^2 \vartheta}\right)\right) \quad \text{and} \quad \frac{1}{z^*} = \frac{1}{z} - \frac{1}{z_{foc}}$$

2. For the beam attenuation in TCV plasmas, a model of hot plasma with a single impurity (with charge number  $Z$ ) has been applied and modified so that only quantities measured at TCV are used as parameters:

$$I(B) = I(A) \exp\left[-\int_A^B \lambda dz\right]$$

$$\text{where } \lambda = n_e \left( \frac{\langle \sigma_e v_e \rangle}{v_b} + \frac{Z - Z_{eff}}{Z - 1} \sigma_{totD} + \frac{Z_{eff} - 1}{Z(Z - 1)} \sigma_{totZ} \right), \quad Z = 6 \text{ at TCV.}$$

The effect of halo (secondary neutrals in the beam vicinity) is not treated for simplicity.

3. The above formulas have been coded into a 3+1 D computer model in MatLab6. The model is able to determine the beam intensity at any point of the beam and at any time even if the TCV plasma position causes large density gradients within the beam volume (cf. Fig. 2). The code, which has been optimised for execution speed, is described in detail in the report [5].

Example of the results of the computer model for both the beam profile in vacuum and the beam attenuation in representative TCV plasmas are presented in fig. 6. The profile edge is limited by the source visibility through the TCV diaphragm. The resulting 3D beam intensity corresponds to the product of the beam vacuum profile and local attenuation value.

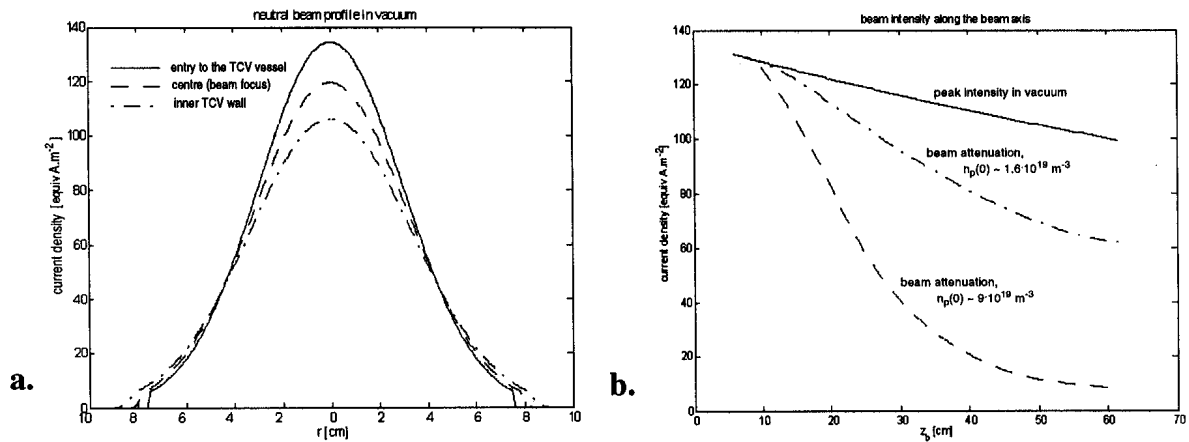


Fig. 6: a. Neutral beam profile in vacuum (pure beam divergence)  
b. Beam attenuation along the beam axis in TCV plasmas

## 5. First experimental results

The first CXRS observations were somewhat disappointing; no active signal was detected from carbon spectroscopy during the DNBI operation. The beam performance and its correct orientation were questioned. Though the beam diagnostics (current and voltage measurements, aiming diaphragm and retractable target data) verified that the beam worked correctly, an independent verification was required. The first obvious method to prove the beam presence and its correct position in the TCV chamber was monitoring of the thermocouples installed at the TCV inner wall. After detailed discussions it turned out that the beam energy content cannot be determined with a sufficient precision from their data, but since the DNBI ion source angular position (azimuth) can be slightly shifted, we could verify the beam position and profile. The beam was fired into evacuated TCV chamber with five different ion source azimuths. The results are shown in figure 7. The circles correspond to the temperature increase at the thermocouple which is positioned vertically at the designed level of the beam axis. The crosses and plusses show the same data for the thermocouples installed 7 mm below and above this level, respectively. The full line correspond to the exponential fit to the circle points, the dashed lines show the same function when shifted by 7 mm. The data prove that the beam had been precisely aimed ( $\Delta z$  of the fit maximum is 3.5 mm). Moreover, from the width of the fitted function and the distance between DNBI grids and thermocouples we could determine the beam divergence, which correspond to  $\vartheta \cong 0.7^\circ$ .

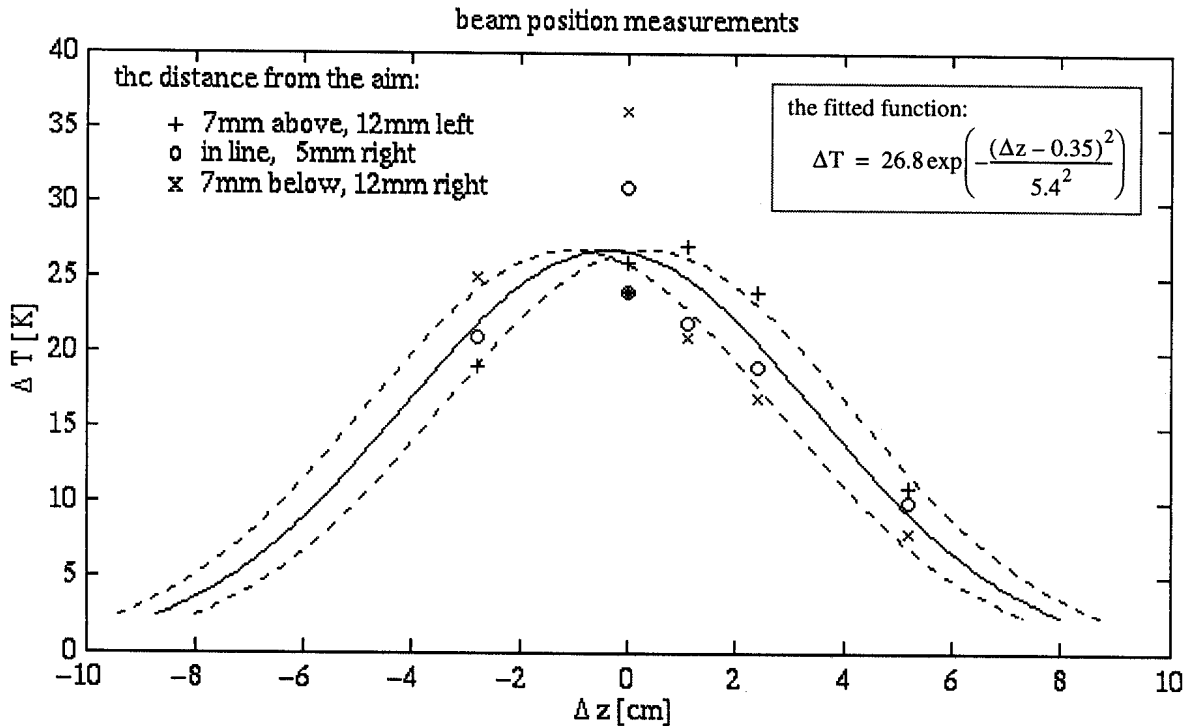


Fig. 7: Beam alignment using the TCV in-vessel thermocouples

The first confirmation of the interaction between the beam neutral particles and the TCV plasma came from the neutral particle analyser (NPA). Namely its high-energy channel (sensitive to neutral atoms with energies 4-7 keV) registered a clear increase in the population of energetic ions in TCV during DNBI operation. They correspond to beam particles which have slowed down to less than 10 keV after their ionization in TCV plasma. A representative example of the NPA high-energy channel data during a TCV discharge and 100/100 ms modulated neutral beam is in fig. 8a. In the same figure the



signal from a single chord measurements of a Doppler-shifted  $H_{\alpha}$  line from the beam in the TCV plasma is presented. The Doppler shift which permitted to isolate the beam signal from the passive emission was high thanks to the fact that the viewing chord was almost parallel to the beam, the angle  $\delta \sim 14^{\circ}$ . Independent measurements proved that the intensity of this signal was almost insensitive to the presence of TCV plasma.

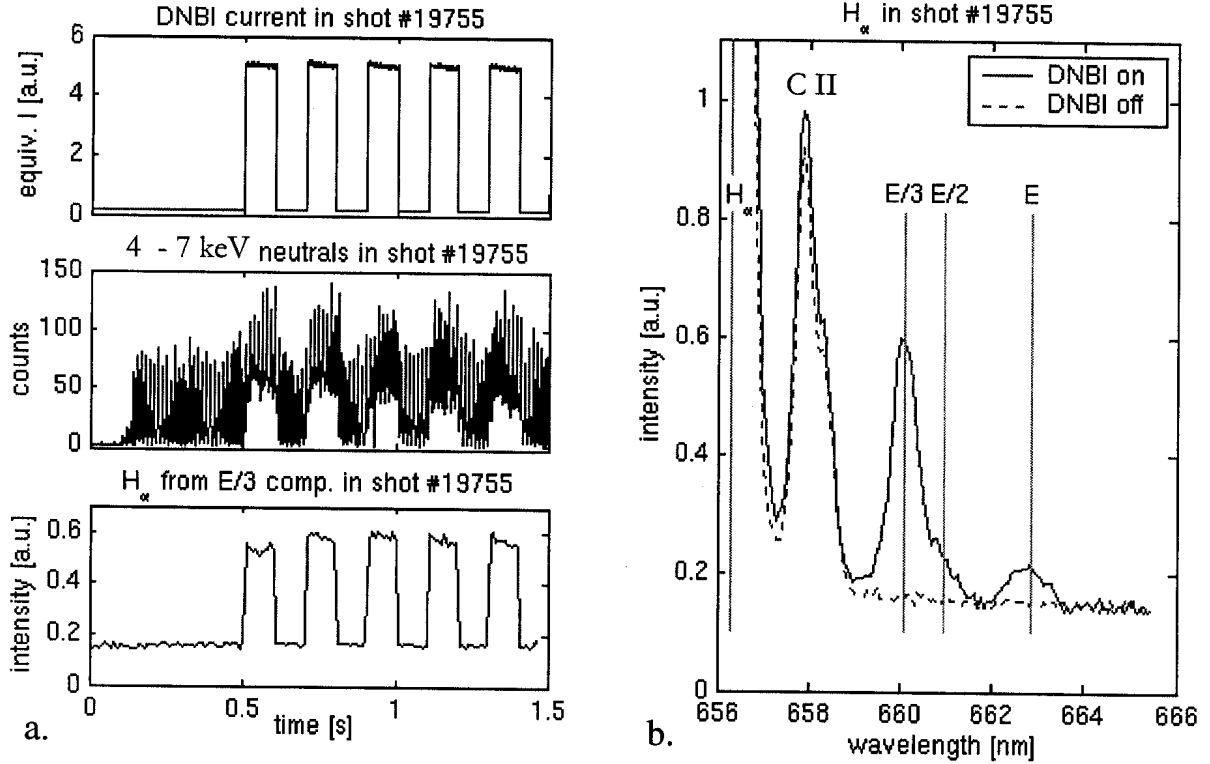


Fig. 8: a. DNBI current, neutral atoms emitted from TCV plasma and doppler-shifted  $H_{\alpha}$  emission along the beam  
 b.  $H_{\alpha}$  emission spectrum: fundamental and three doppler-shifted DNBI components

The spectral measurements of the  $H_{\alpha}$  emission are presented in fig. 8b. They give evidence of the three beam components as mentioned in section 2. From the Doppler shift value

$$\lambda' = \lambda_{H_{\alpha}} \left( 1 + \frac{1}{c} \sqrt{\frac{2E}{m}} \cos \delta \right)$$

where  $\lambda_{H_{\alpha}} = 656.3$  nm we calculate that the most shifted line (662,8 nm) corresponds to the particle energy  $E = 50$  keV, while the 660.9 nm and 660.1 nm correspond to the beam components with  $E/2$  and  $E/3$ , respectively.

The intensities of the three lines were compared using the time integral of the spectral measurements. The obtained ratio between E, E/2 and E/3 line intensity is 5.2 : 14 : 29. Taking into account the cross-sections ratio for  $H_{\alpha}$  charge-exchange at the given energies (1 : 3.3 : 5.6) and decrease of beam particle density with current velocity we found that the above line intensity ratio correspond to beam current density ratio 47 : 26 : 27. In other words, though the E/3 feature is much more intense than the full energy feature, a rough estimate of the beam components ratio in principle agrees with the expected ratio 36 : 31 : 18 presented in sec. 2. The low resolution of the spectrometer used may account for the difference; a more sensitive spectrometer is foreseen for future  $H_{\alpha}$  measurements.

It is to be noted however that there is little general interest in measurements with the diagnostic chord almost parallel to the beam. The major task of the diagnostic beam is to perform local measurements in the plasma, in which case the viewing lines must be nearly perpendicular to the beam, see the case of the CXRS diagnostic set-up (fig. 2). That is why it was imperative to detect the beam using the CXRS system. Eventually, after increasing of the spectrometer sensitivity, the charge exchange processes along the beam were registered by CXRS, see fig. 9. The left part of the figure presents CXRS spectra of the CVI  $n=8 \rightarrow 7$  transition with integration time 50 ms and along viewing line 5 cm off the plasma centre. The width of the Gaussian fitted on the active signal correspond to line Doppler broadening at  $T_i = 520$  eV. However, the active signal is far too low and noisy to determine the ion temperature reliably. In the right part of the figure, the measured active / passive signal level ratios for different plasma densities are outlined. Obviously, reasonable values can be obtained only when TCXV operates at atypically low plasma densities.

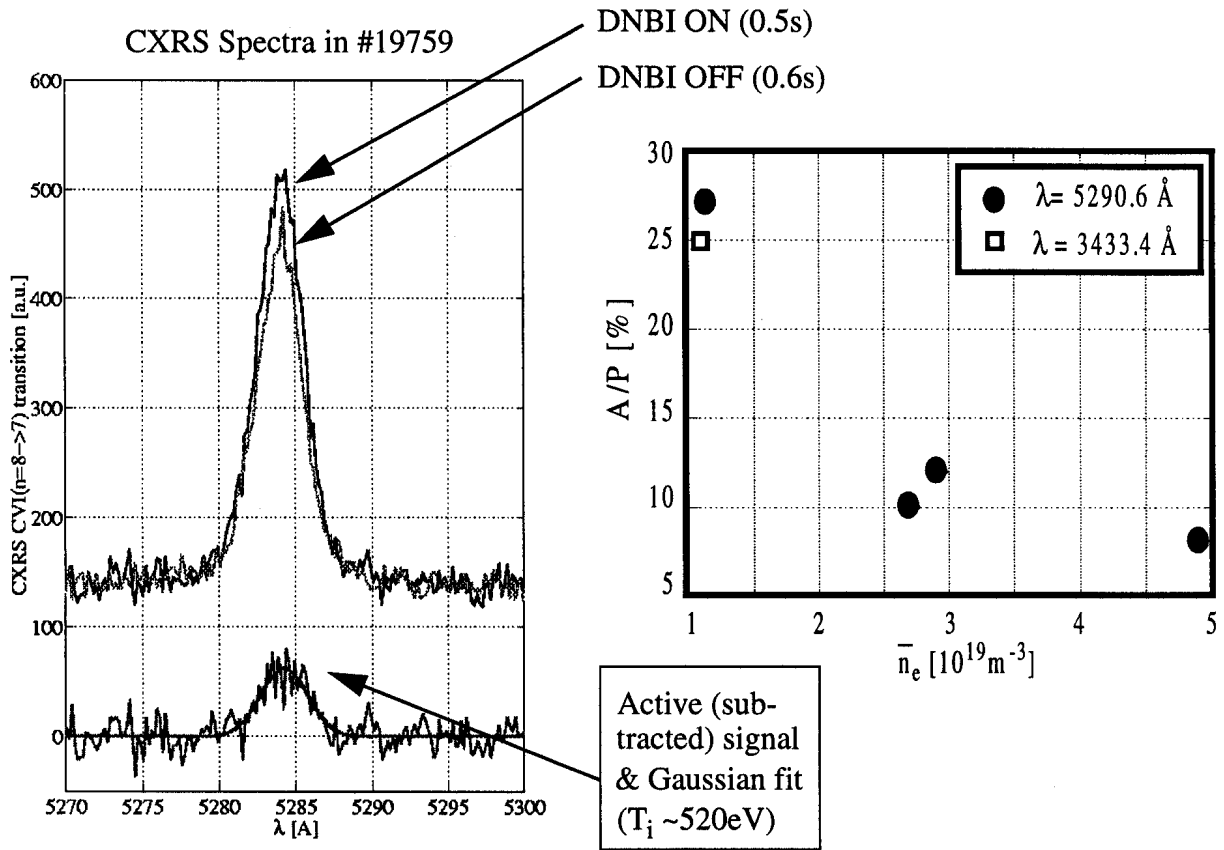


Fig. 9: First results of CXRS measurements with modulated neutral beam

Consequently, it became clear that the DNBI-CXRS diagnostic system cannot be applied in its present set-up for the expected purpose due to unexpected high passive emission of the TCXV plasmas. The problem has been studied in detail in ref. [6]. In conclusion, two major upgrades will be installed in near future:

1. The photon statistics of CXRS will be substantially improved so that even low active signal can be reliably measured. In other words, the CXRS system will be upgraded to increase its signal to noise ratio approximately by a factor of five. This will be achieved by increasing the number of optical fibres, by installing monochromators with higher aperture and higher reflectivity gratings as well as by using back-illuminated CCD cameras.

2. The active over passive signal ratio will be increased. The only realistic possibility is to upgrade DNBI so that it could deliver higher beam current density, hopefully by up to a factor of three. In the first phase of the planned upgrade enforcing the HVM power will increase the extracted current. The upgraded injector will then be able to work only in modulated regime, as the necessary power will be

supplied partly by a capacitor bank which stores the electrical energy available between pulses. This energy was previously dumped into a bank of resistors but we cannot keep to this principle because of the mains supply current limits. The RF power source will be modified to deliver higher power, too, and the surface of the grids will be enlarged. In the second phase the injector line may be shortened (a shrunk vacuum tank with a single cryopump will be applied) and the grids will be refocussed so that the resulting beam is narrower.

The upgrade should be finished in 2002, but first improvements are expected in 2001.

## 5. Conclusions, acknowledgements

The diagnostic neutral beam, which has been commissioned on TCV in 2000, presents a particularly complex but promising diagnostic system. A new DNBI remote control system has been developed and model of beam profile and attenuation has been coded. First experimental results have proven correct beam performance.

Unfortunately, the first CXRS measurements have shown that little useful data can be acquired with the given neutral beam density at normal TCV operation densities due to unexpectedly high passive emission of TCV plasmas. As a result, both the CXRS system and the DNBI will be upgraded in order to increase the signal to noise ratio and the active to passive signal ratio, respectively.

The authors appreciate the support of both the TCV and BINP groups.

The work has been partly supported by the Swiss National Science Foundation.

This report can be found online at the following website:

<http://crppwww.epfl.ch/~mlynar/doc/>

## 6. References

- [1] H. Weisen and TCV Team: *Overview of TCV Results*  
invited talk OV5/1, 18th IAEA Fusion Energy Conference, Sorrento, Italy, October 2000  
[http://crppwww.epfl.ch/conferences/IAEA00/tcv\\_paper.pdf](http://crppwww.epfl.ch/conferences/IAEA00/tcv_paper.pdf)  
and references therein
- [2] W. Mandl, R.C. Wolf, M.G. von Hellermann and H.P. Summers: *Beam Emission Spectroscopy as a comprehensive Plasma Diagnostic Tool*  
Plasma Phys. Control. Fusion **35**, 1373 (1993)
- [3] F.M. Levinton: *The motional Stark effect: Overview and future development*  
Rev. Sci. Instrum. **70**, 810 (1999)
- [4] A.A. Ivanov et al: *Radio frequency ion source for plasma diagnostics in magnetic fusion experiments*  
Rev. Sci. Instrum. **71**, 3728 (2000)
- [5] J. Mlynar: *TCV DNBI Profile and Attenuation Studies with Code Manual*  
LRP 692/01, CRPP EPFL, Lausanne 2001  
[http://crppwww.epfl.ch/~mlynar/doc/dnbi\\_lrp692.pdf](http://crppwww.epfl.ch/~mlynar/doc/dnbi_lrp692.pdf)
- [6] P. Bosshard, B.P. Duval, J. Mlynar, H. Weisen: *Charge Exchange Recombination Spectroscopy Optimisation with the TCV Diagnostic Neutral Beam*  
28th EPS Conference on Controlled Fusion and Plasma Physics, Madeira, Portugal 2001  
[http://crppwww.epfl.ch/conferences/EPS01/pb\\_paper.pdf](http://crppwww.epfl.ch/conferences/EPS01/pb_paper.pdf)